

# A Monolithic Array of 77 Silicon Drift Detectors for X-ray Spectroscopy and Gamma-ray Imaging Applications

C. Fiorini, M. Bellini, A. Gola, A. Longoni, F. Perotti, P. Lechner, H. Soltau, L. Strüder

**Abstract**— Monolithic arrays of Silicon Drift Detectors (SDDs) have been employed successfully in X-ray spectroscopy and  $\gamma$ -ray imaging applications. Thanks to the low electronics noise achieved at short shaping time, the SDD is an ideal device for high-resolution and high-rate X-ray spectroscopy experiments at synchrotron sources. Moreover, small monolithic arrays of SDDs have also been used as photodetector of the scintillation light in a first prototype of Anger Camera for  $\gamma$ -ray imaging characterized by an intrinsic resolution better than 0.3mm. In this work we present a new large-area monolithic array of Silicon Drift Detectors. It consists of a single chip composed by 77 single hexagonal units, each one with a front-end JFET integrated in its center, arranged in a honeycomb configuration. Each SDD unit has an active area of 8.7mm<sup>2</sup>, for a total active area of the device of 6.7cm<sup>2</sup>. The linear dimensions of the active area are approximately 28×24mm<sup>2</sup>. It represents the largest monolithic array of SDDs with on-chip JFETs produced up to now for X-ray and  $\gamma$ -ray detection. The results achieved in the experimental characterization of a first prototype of the detector array are presented. They include also the preliminary X-ray spectroscopy characterization of the SDDs units. The energy resolution measured at 6keV with the single unit of the array is of 142 eV at -10°C.

## I. INTRODUCTION

Silicon Drift Detectors (SDDs) are employed successfully in an increasing range of applications in the field of X-ray Spectroscopy. Thanks to the low output capacitance (in the order of 100fF) independent from the area, and to the integration of the front-end JFET on the detector chip [1], these detectors are characterized by a much lower electronics noise with respect to conventional photodiodes of the same area and thickness. Moreover, the best electronics noise is

achieved at short shaping time (less than 1 $\mu$ s), a feature that makes these devices ideal for high-counting-rate applications.

Monolithic arrays of SDDs are of particular interest in high-resolution and high-rate X-ray Spectroscopy in synchrotron applications like XAFS (X-ray Absorption Fine Structure) experiments [2] and X-ray holography. In fact, taking into account the already high-counting-rate capability of the single SDD unit (few hundreds kcounts/s for a typical area of 5mm<sup>2</sup>), the use of several units integrated in a segmented detector of relatively large area (few cm<sup>2</sup>) could allow to achieve a counting capability of the whole detection system up to tens of Mcounts/s.

Moreover, monolithic arrays of SDDs have been recently experimented also for the development of Anger Cameras for high-resolution  $\gamma$ -ray imaging [3]. In this application, the SDD is employed as the photodetector of the scintillation light emitted by a crystal which has absorbed the  $\gamma$ -ray. Superior performances have been achieved with respect to the conventional scintillation readout operated by means of photomultiplier tubes (PMTs). In a first prototype of a small Anger Camera, a SDD array of 1cm<sup>2</sup> active area has been coupled to a single CsI(Tl) scintillator. An intrinsic spatial resolution better than 0.3 mm FWHM has been measured with this prototype, almost one order of magnitude better than the performances achievable with conventional Anger Cameras based on PMTs.

In all mentioned applications, monolithic arrays have been limited up to now to small areas (max. 1cm<sup>2</sup>) composed by a limited number of units. Although these detectors have shown to provide good performances, a quite challenging technological goal is to demonstrate the feasibility of producing larger monolithic arrays of SDDs, with an area in the order of several cm<sup>2</sup>, composed by several tens of units.

In this work we present a new large-area monolithic array of 77 SDDs. The detector has been developed in the framework of the project DRAGO, supported by Italian INFN. The goal of the project is to develop a gamma-ray imager characterized by a submillimeter position resolution, to be used either for specialized medical imaging applications and for small animal imaging.

The detector here presented is characterized by an active area of about 6.7 cm<sup>2</sup> which makes it the largest monolithic array of SDDs with on-chip JFETs produced up to for this kind

---

Manuscript received November 15, 2004. This work was supported by Italian INFN (Experiment DRAGO).

C. Fiorini, M. Bellini, A. Gola and A. Longoni are with Politecnico di Milano, Dipartimento di Elettronica e Informazione, and with INFN – Sezione di Milano, Milano, Italy. (telephone: +39-02-23993733, e-mail: carlo.fiorini@polimi.it).

F. Perotti is with Istituto di Astrofisica Spaziale e Fisica Cosmica - INAF Sez. ‘G. Occhialini’, Milano, Italy.

P. Lechner and H. Soltau are with PNSensor GmbH, München, Germany.

L. Strüder is with MPI für Extraterrestrische Physik Halbleiterlabor, München, Germany.

of applications. To achieve this result, new technological issues had to be addressed in the fabrication technology. Among them, the most relevant is represented by a new scheme of interconnections of the single units for the extraction of the bias and signal lines.

A suitable hybrid has been realized to mount and connect the detector. The detector has been first electrically characterized to qualify the technology process. Then, after mounting a first prototype on the hybrid substrate, it has been also tested in spectroscopy measurements by means of a  $^{55}\text{Fe}$  source. The preliminary results obtained are here reported. These includes either in the characterization of the noise performances of the single unit and the evaluation of the uniformity of performances of all the units of the array on this first prototype.

## II. THE MONOLITHIC ARRAY OF 77 SDD CELLS

The detector presented here has been produced at the Semiconductor Laboratory of the Max Planck Institut of Munich (Germany). The layout of the array is shown in Fig.1. It consists of a single chip composed by 77 single hexagonal units, each one with an active area of  $8.7\text{mm}^2$ , for a total active area of  $6.7\text{cm}^2$ . The chip size is  $36\times 32\text{mm}^2$ . The linear dimensions of the active area are approximately  $29\times 26\text{mm}^2$ . Although a square shape for the single unit would have allowed a more effective filling of the rectangular area, an hexagonal geometry has been chosen because more experimented in previous arrays with respect to a completely new square-like geometry. With respect to previous productions of SDD devices, the wafer thickness has been increased from  $300\mu\text{m}$  to  $450\mu\text{m}$  for the present device, allowing a higher quantum efficiency for X-ray detection. The increase of the active volume has not caused an increase of the leakage current with respect to previous devices, thanks to the improvements achieved in the meantime in the fabrication technology.

Each SDD has a n-channel JFET integrated in the center of the unit, internally connected to the anode ring. In a standard SDD, the bonding pads for the connections of the transistor electrodes as well as for the other electrodes of the device were placed in the central region of the unit. The possibility of extracting the bonding pads outside the active area of the device was prevented by the fact that the connecting strips to these electrodes should have crossed the drift rings of the device, biased at high voltages. The passivation layer between metal and ring electrodes would not have held such a voltage difference. The limited number of units monolithically assembled in previous small arrays allowed to find reasonable hybrid solutions for the contact of all bonding pads inside each unit. However, the perspective of connecting the bonding pads placed at each SDD center in a large array like the one shown in Fig. 1a, appeared a task almost impossible to be accomplished.

For this reason, thanks to new availability of two interconnecting layers (polysilicon and aluminum) in the fabrication technology, in the present detector all signals and biasing lines have been extracted from the centre of each unit to the external regions of the chip. As shown in Fig. 1a, the

connections to the internal electrodes are aligned in buses and are provided to a series of bonding pads on the outer regions of the chip, in a similar way to the connection scheme employed in conventional integrated circuits.

The back-side of the detector consists of an homogeneous entrance window for the radiation (Fig. 1b). Bonding pads are placed at the corners outside the active area in order to allow the coupling of a scintillator without interfering with the bonding wire. A suitable anti-reflective coating structure has been implemented on the backside to achieve a photon transmission higher than 80% between 400nm and 650nm.

For mounting and bonding of the SDD array, a suitable ceramic holder has been designed. The detector mounted on the holder is shown in Fig. 2a. For the detector assembly, the idea was to exploit the new opportunity of having the front-side of the detector (Fig.1a) free from bonding connections in the active region of the device. Accordingly, in order to keep the cross section of the detection module as much as possible limited only by the chip dimensions, a hybrid has been designed to be mounted on the inner region of the detector front-side. In this way, bonding connections are provided from the bonding pads on the chip towards pads on the outer regions of the hybrid. A detail of the bondings is shown in Fig. 2b. The signal and bias lines from the detector are extracted by means of two connectors placed on the hybrid. From Fig.2a it can be also noted that between the two connectors on the hybrid, room is still available to thermally connect the hybrid with a Peltier cooler. It is planned to cool the hybrid module to about  $-10^\circ\text{C}$ . For this purpose, the hybrid has been realized in a high-thermal conductive material such Aluminum Nitride (Alunit). No relevant modifications of the electrical characteristics of the detector (presented in the next paragraph) have been observed after the assembly of the hybrid on the chip.

## III. ELECTRICAL CHARACTERIZATION

An electrical characterization of the 77-SDDs detector has been carried out on three prototypes. Similar electrical characteristics have been measured on all three devices.

In Fig. 3, the measurement of the leakage current carried out on the detector held at room temperature is reported. At the depletion voltage, about  $-70\text{V}$ , a current of  $4\text{nA}$  was measured, which corresponds to an area-scaled value of  $0.6\text{nA}/\text{cm}^2$ .

In Fig. 4, the electrical characteristic of the integrated voltage divider is also reported. The voltage divider is obtained by means of a sequence of resistors, each one integrated between two adjacent rings. The biasing of the drift rings of the detector is therefore achieved only by applying a voltage difference between first and last ring.

The meaning of the result shown in Fig.4 is not only limited to the verification of the correct operation of the integrated voltage divider. In fact, it has to be noted that the measurement has been carried out by applying up to  $-150\text{V}$  between the last ring and the first ring of the device. The first ring voltage is applied to an external pad of the device which is connected to the corresponding electrode by means of a metal strip crossing the last ring electrode, as well as the whole active area of the

unit. Therefore, the test demonstrates also that the lines crossing the high-voltage rings of the detector (see the region highlighted in the layout shown in Fig.5) can stand a high voltage difference with respect to the most negative electrode, without any breakdown occurring.

The characteristics of all 77 JFETs have also been tested on the three available devices. Fig. 6 shows the current measured by applying a voltage difference between drain and source of all the integrated transistors on a prototype. All JFETs could be operated and show good characteristics. The maximum deviation of the measured currents is of 14%. This deviation is not critical for the readout electronics which is based on the operation of the transistors in a source follower configuration by means of external current sources. The correct operation of all 77 JFETs was verified also on the other two prototypes.

#### IV. X-RAY SPECTROSCOPY CHARACTERIZATION

In order to evaluate the spectroscopy performances offered by the SDD array, a suitable experimental setup has been realized. The detector is connected by means of two flex cables plugged into the hybrid connectors, as shown in Fig. 7. The flex cables were then plugged into a PCB which allowed the biasing of all detector electrodes and JFETs. The outputs of the JFETs were fed into a preamplifiers board which allowed to monitor contemporaneously the signals at the output of a limited number of units. A CMOS chip for the readout of the complete 77 SDDs array is under development [4].

The basic schematic of the preamplifier used for readout of the SDD signal is reported in Fig. 8. Each source follower is followed by a voltage preamplifier realized by means of a coupling capacitor followed by a charge preamplifier. The preamplifier output is then processed by means of a semigaussian shaping amplifier, a Tennelec Tc244 in our case. Particular care has been taken in the evaluation of possible cross talks between neighboring channels. In fact, the output lines of channels grouped in common buses, as shown in Fig. 1a, could be in principle slightly capacitively coupled. Moreover, output lines of contiguous channels could not be prevented to run close each other also on the hybrid shown in the photo of Fig.2a (these lines are only partially visible in the photo because of an overlapped passivation layer). A cross-talk capacitance between contiguous channels has been evaluated to be of the order of few pF in the worst case, and is symbolically shown in Fig.8. The cross talk was expected to be minimized by the fact the signal induced from one channel to the neighbor channel through the cross-talk capacitance is applied to the low output impedance of the source follower stage ( $1/g_m \sim 3k\Omega$ , being  $g_m$  the JFET transconductance). Considering the shaping waveforms to be used in the spectroscopy measurements and the values of the device parameters of the front-end electronics, a cross talk smaller than  $10^{-3}$  between two contiguous channels has been evaluated by simulations. The level of cross-talk between contiguous channels has been also experimentally verified. In Fig. 9, the output waveforms from the preamplifier of the two channels are shown during the detection of X-ray events from a  $^{55}\text{Fe}$  source. From the figure it can be observed

that when one of the two channels process an event, no noticeable cross-talk signal appears on the other channel, in agreement with the predictions.

One detector prototype among the three electrically tested was fully characterized in spectroscopy measurements by means of a  $^{55}\text{Fe}$  source. The detector was cooled down to  $-10^\circ\text{C}$  by means of a climatic chamber. In Fig. 10 the  $^{55}\text{Fe}$  spectrum measured with a single unit of the array is shown. At the Mn-K $\alpha$  line, the energy resolution is of 142eV FWHM, corresponding to an electronics noise of 9.2 e-rms, using 0.75 $\mu\text{s}$  shaping time. This performance is rather remarkable for a detector unit of 8.7mm<sup>2</sup> active area operated with a moderate cooling. Because not all the channels could be monitored contemporaneously by an adequate number of preamplifiers, a limited number of detector units were tested at  $-10^\circ\text{C}$  and they have shown similar resolution performances with respect to the one reported above.

The spectroscopy performances were evaluated also using different shaping times. A graph of the ENC versus shaping time is reported in Fig. 11. It can be noted that at the shaping times to be used for the photodetection of CsI(Tl) scintillation light (decay time of about 1 $\mu\text{s}$ ), the electronics noise is still satisfactory. For instance, at a shaping time of 4 $\mu\text{s}$ , the ENC, although worse of almost 50% with respect to the optimum value is still 15e-rms. In order to get the best performance achievable with the SDD with the shaping time in the order of 1 $\mu\text{s}$ , crystal scintillators with a light output similar to CsI(Tl) but with a much lower decay time should be employed. The recently discovered LaBr<sub>3</sub> scintillator [5] seems to be a good option to be explored, thanks to its decay time of only 25ns and a light output of about 60000 photons/MeV, similar to the one CsI(Tl).

In order to verify the possibility to bias all 77 units with a common set of voltages,  $^{55}\text{Fe}$  spectra were acquired at room temperatures from all the SDDs. Concerning specifically this point it has to be mentioned that not all the electrodes of each unit could be accessed externally with a custom bias. Most of the bias voltages, in fact could be provided commonly to all units by means of bias lines running around the active area of the device (visible in Fig.1a). A minimal degree of freedom was kept by the division of the 77 SDDs in ten groups of 7 and 8 units, each group with a separated voltage for the first drift ring R#1. During the spectroscopy measurements carried out at room temperature, three units of the array stopped to work for reasons still unknown. The other units were first biased one at a time with a custom first ring voltage, in order to first verify their best performances. While doing so, all 74 operated units showed good spectra with very good noise performances at room temperature. However, when we tried to bias contemporaneously all the units using a unique R#1 bias common only for each single group of 7-8 units, the result was that 59 SDDs (80% among 74 units) still showed good spectra while 15 SDDs (20%) showed spectra more or less affected by problems of partial charge collection. The bias of R#1 resulted critical to guarantee a proper collection of the charge toward the anode. A characterization extended to the other available

prototypes, which are in the phase of being assembled and bonded on the hybrids, is required to better verify this limitation. Moreover, to better evaluate the lack of performances derived from the limited charge collection efficiency observed on the 15 units, we intend also to further investigate the device by irradiating the full area of each unit by visible light, a condition much more similar to the scintillation photodetection with respect to the localized absorption of X-rays. Depending on the results obtained in these further tests, the uniformity limitation could be addressed in a second production of the detector where improved doping profile will be implemented to keep performances more independent from the detector biasing.

## V. CONCLUSIONS

In this work we have presented a new monolithic array of 77 SDDs to be used for high-rate X-ray Spectroscopy applications as well as for  $\gamma$ -ray imaging with scintillators. The results of the experimental characterization of a first prototype of the detector show that the electrical characteristics of the detector are satisfactory and all the 77 JFETs integrated on the detector chip are operating properly. The noise performances measured at the level of single SDD unit by irradiation with a  $^{55}\text{Fe}$  source are very good for the potential applications of the array in high-resolution spectroscopy and  $\gamma$ -ray imaging. The homogeneity of performances with a common biasing of the different units has been demonstrated to be only partially achieved with this first prototype. This feature has to be

verified on the other available prototypes as well as in measurements with visible photons. A second production of the detector is already planned to overcome the present limitations.

## VI. ACKNOWLEDGMENTS

The authors would like to thank C. Turconi for the help during the measurements.

## VII. REFERENCES

- [1] P. Lechner, C. Fiorini, R. Hartmann, J. Kemmer, N. Krause, P. Leutenegger, A. Longoni, H. Soltau, D. Stötter, R. Stötter, L. Strüder, U. Weber, "Silicon drift detectors for high count rate X-ray spectroscopy at room temperature", *Nucl. Instr. and Meth.*, A 458, 281-287, 2001.
- [2] Ch. Gauthier, J. Goulon, E. Moguiline, A. Rogalev, P. Lechner, L. Strüder, C. Fiorini, A. Longoni, M. Sampietro, H. Besch, R. Pfitzner, H. Schenk, U. Tafelmeier, A. Walenta, K. Misiakos, S. Kavadias, D. Loukas, "A high resolution, 6 channels, Silicon Drift Detector Array with integrated JFETs designed for XAFS spectroscopy: first X-ray fluorescence excitation spectra recorded at the ESRF", *Nucl. Instr. and Meth.*, A 382, 524-532, 1996.
- [3] C. Fiorini, A. Longoni, F. Perotti, C. Labanti, E. Rossi, P. Lechner, H. Soltau, L. Strüder, "A monolithic array of silicon drift detectors coupled to a single scintillator for  $\gamma$ -ray imaging with sub-millimeter position resolution", *Nucl. Instr. Meth.*, Vol. A512, pp. 265–271, 2003.
- [4] C. Fiorini, M. Porro, "DRAGO chip: a low-noise CMOS preamplifier-shaper for Silicon Detectors with on-chip JFET", Proceedings of the IEEE-Nuclear Science Symposium 2004, submitted to *IEEE Trans. Nucl. Science*.
- [5] E.V.D. van Loef, P. Dorenbos, C.W.E. van Ejik, K. Kramer and H.U. Gudel, "High resolution scintillator:  $\text{Ce}^{3+}$  activated  $\text{LaBr}_3$ ", *Appl. Phys. Lett.*, vol.79, pp. 1573-1575, Sep.2001.

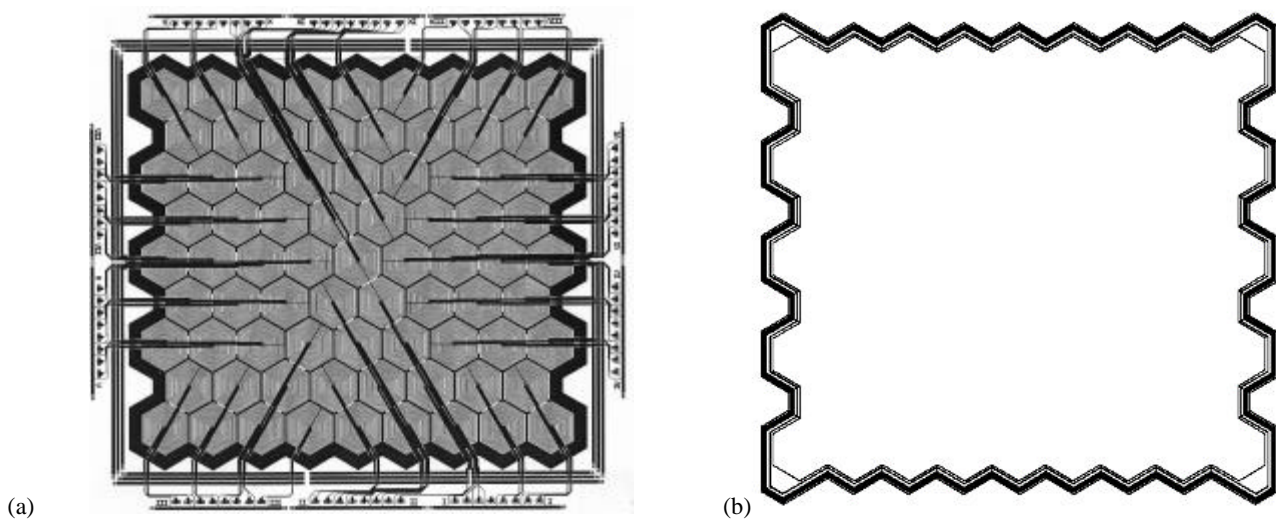


Fig. 1. Layout of the monolithic array of 77-SDDs. The detector side where the drift rings and the front-end JFET are integrated is shown in the figure (a). The entrance window for X-rays of scintillation photons is the opposite side of the detector (b).

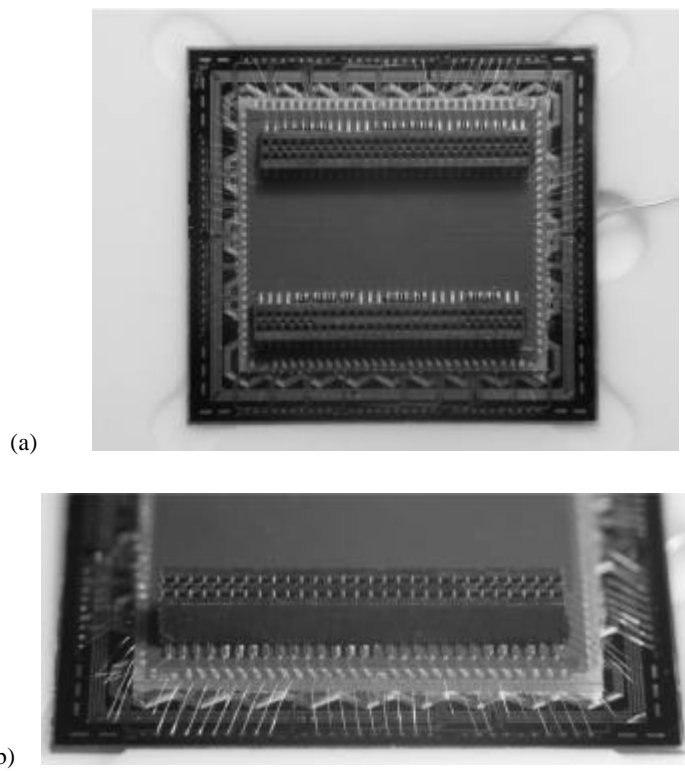


Fig. 2. (a) Mounting of the hybrid on the front side of the monolithic array. (b) Detail of the bonding connections.

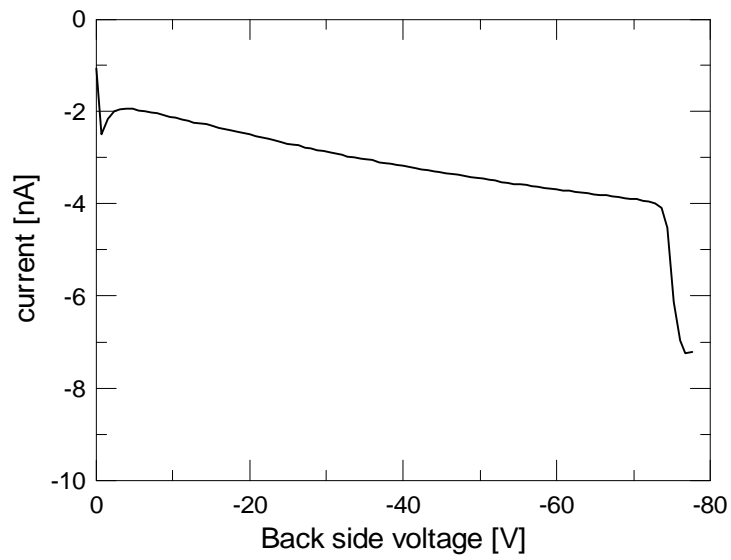


Fig. 3. Measurement of the leakage current on the back side of the detector, common to all units.

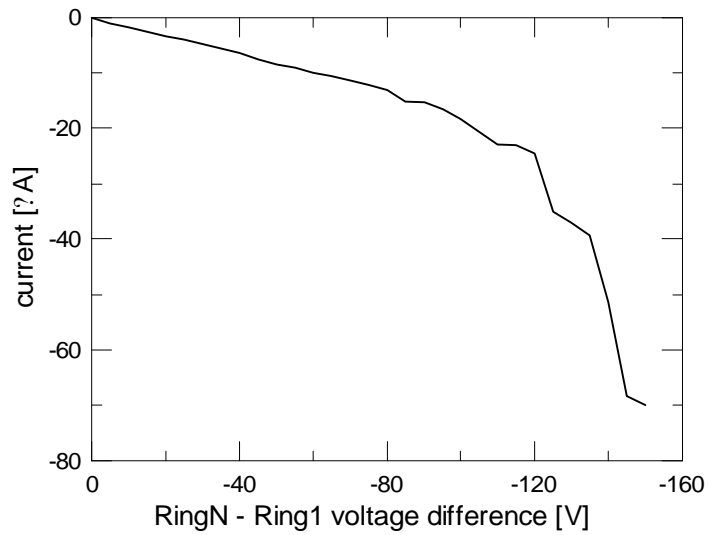


Fig. 4. Electrical characteristic of the integrated voltage divider implemented for the biasing of the SDD drift rings through only the application of voltages to the last and first rings.

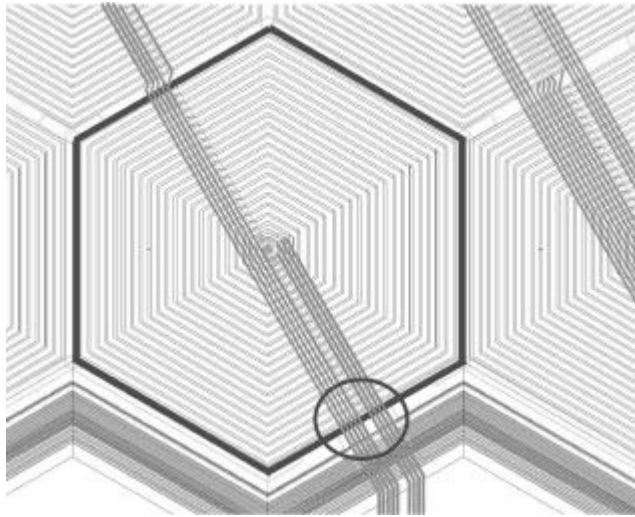


Fig. 5. Detail of the layout of a single SDD unit in the monolithic array. A region where the low-voltage bias lines are crossing the outermost ring (identified in the figure by the dark contour), biased at high voltage, is highlighted.

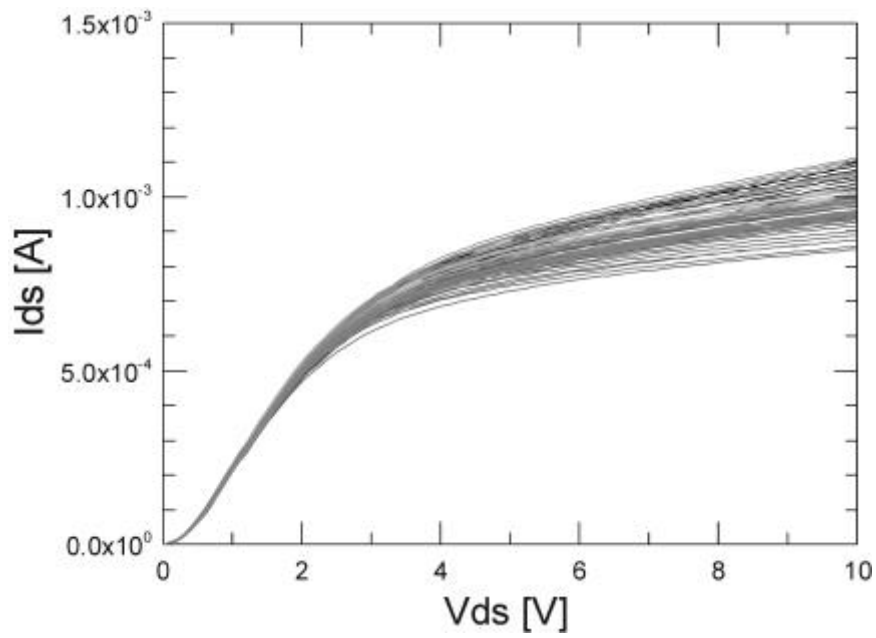


Fig. 6. Characteristics of the 77 on-chip JFETs.



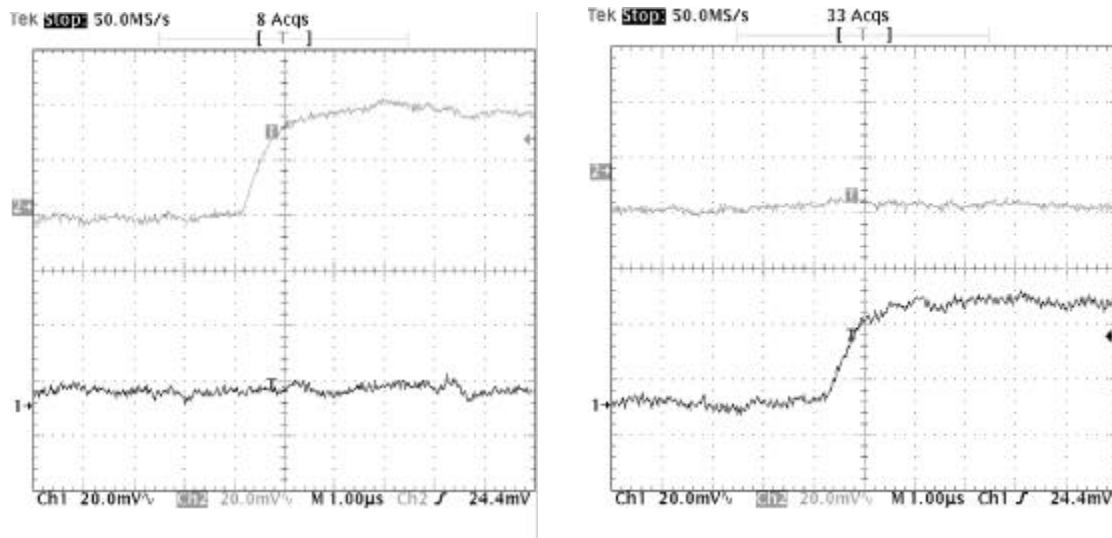


Fig. 9. Preamplifier signals measured on two contiguous channels. When one of the two channels is hit by a  $^{55}\text{Fe}$  signal, no noticeable cross-talk signal is detected by the other channel.

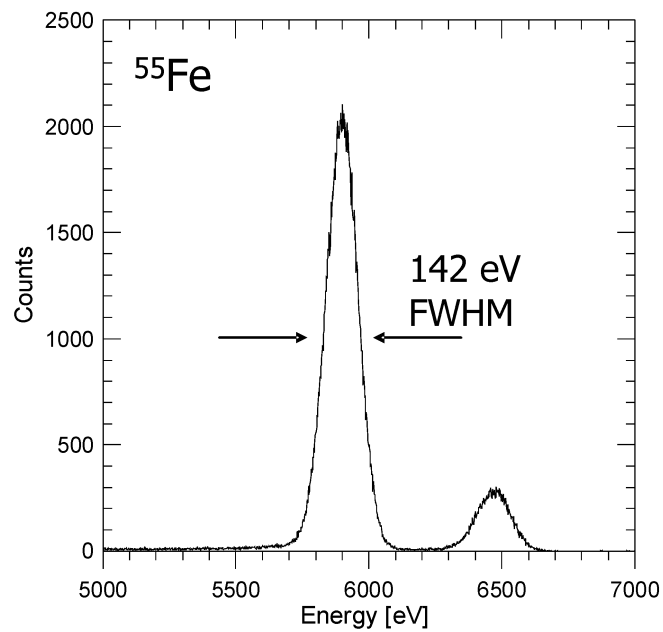


Fig. 10.  $^{55}\text{Fe}$  spectrum measured on a single unit of the array at  $-10^\circ\text{C}$  and using a shaping time of  $0.75\mu\text{s}$ .

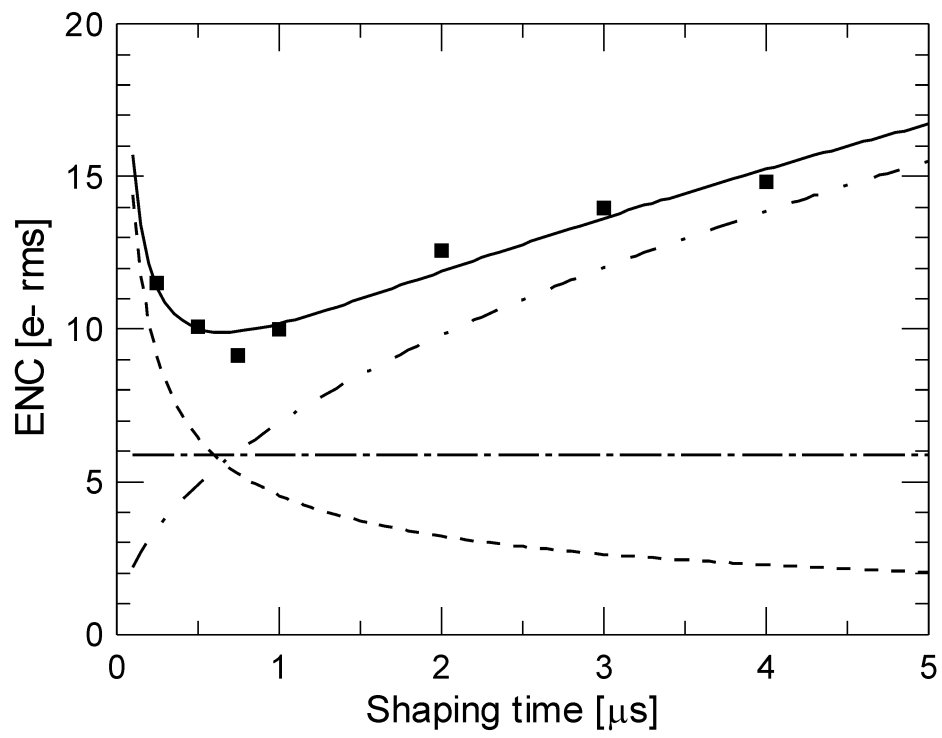


Fig. 11. ENC versus shaping time, measured at  $-10^{\circ}\text{C}$ .